Table 1. Antibodies used in the current study and their positive rates in 870 GCs

Antibody	Clone	Dilution	Source	Positive cases n (%)
CK7	OV-TL 12/30	1:50	DAKO, Carpinteria, Calif., USA	648 (74)
CK20	IT-Ks 20.8	1:50	DAKO, Carpinteria, Calif., USA	232 (27)
MUC5AC	CLH2	1:50	Novocastra, Newcastle, UK	519 (60)
MUC6	CLH5	1:50	Novocastra, Newcastle, UK	233 (27)
MUC2	Ccp58	1:50	Novocastra, Newcastle, UK	199 (23)
CD10	56C6	1:50	Novocastra, Newcastle, UK	71 (8)
p53	DO-7	1:50	Novocastra, Newcastle, UK	293 (34)
EGFR	EGFR.113	1:50	Novocastra, Newcastle, UK	109 (13)
CDX2	AMT28	1:20	BioGenex, San Ramon, Calif., USA	183 (21)
β-Catenin	14/β-catenin	1:50	BD Biosciences, San Jose, Calif., USA	140 (16)

The cutoff point for antibody reactivity necessary to define a result as positive was staining of at least 10% of cancer cells in the TMAs.

20 min to block nonspecific antibody binding sites. Sections were then incubated with the following primary antibodies: anti-CK7, anti-CK20, anti-MUC5AC, anti-MUC6, anti-MUC2, anti-CD10, anti-p53, anti-EGFR, anti-CDX2 and anti-β-catenin. Suppliers and working dilutions are noted in table 1. Sections were incubated with a primary antibody for 1 h at 25°C, followed by incubations with peroxidase-labeled anti-rabbit or mouse IgG for 60 min. Staining was completed with a 10-min incubation with the substrate-chromogen solution. The sections were counterstained with 0.1% hematoxylin. Appropriate positive and negative control samples were used.

Evaluation of Positive Cases and Cutoff-Point Thresholds

Immunostaining results were evaluated independently by 3 investigators (H.T., K.S. and M.M.) and when the evaluations differed, a decision was made by consensus while the investigators reviewed the specimen with a multihead microscope. Neoplastic tissue was evaluated semiquantitatively at magnifications of ×100 and ×400. Cytoplasmic immunoreactivity for CK7, CK20, MUC5AC, MUC6 and MUC2, membranous reactivity for CD10 and EGFR, and nuclear reactivity for p53, CDX2 and β-catenin were assessed (fig. 1). The cutoff point for antibody reactivity necessary to define a result as positive was staining of more than 10% tumor cells in the TMAs.

CK Expression Profiles and Mucin Phenotypes

The 870 GCs were evaluated according to the CK7 and CK20 staining pattern and classified into four main groups: (1) coexpression of CK7 and CK20 (CK7+/CK20+), (2) no expression of CK7 and CK20 (CK7–/CK20–), (3) only CK7 expression (CK7+/CK20–) and (4) only CK20 expression (CK7–/CK20+). The criteria [24] for classification of G type and I type were as follows: GCs in which more than 10% of the cells displayed the gastric (MUC5AC and/or MUC6) or intestinal epithelial cell phenotype (MUC2 and/or CD10) were G type or I type, respectively. Those sections that showed both G and I types were classified as GI type, and those that lacked both G and I types were classified as N type.

Statistical Methods

Associations between CK expression profiling and clinicopathologic variables, or immunostaining for various markers were analyzed by the χ^2 test. $p < 0.001$ was considered statistically significant.

Results

CK Expression Patterns in GCs and Their Correlation with Clinicopathologic Parameters

Immunohistochemical results in the current study are shown in table 1. The 870 GCs included 648 (74%) cases with CK7 expression and 232 (27%) cases with CK20 expression, and were classified into 156 (17%) cases with CK7+/CK20+ pattern, 492 (57%) cases with CK7+/CK20– pattern, 76 (9%) cases with CK7–/CK20+ pattern and 146 (17%) cases with CK7–/CK20– pattern. We investigated the relation between CK expression patterns and the clinicopathologic parameters including age, sex, tumor location, T grade, N grade, M grade, staging and histological type according to the Lauren classification. As shown in table 2, the CK7–/CK20– pattern was observed more frequently in the diffuse type of GC than in the intestinal type ($p = 0.0003$). In contrast, no differential trend was found between other CK expression patterns and clinicopathologic parameters. Regarding the Japanese Classification of Gastric Carcinomas, the CK7–/CK20– pattern was observed more frequently in the undifferentiated type (por1, por2, sig and muc) than in the differentiated type GC (pap, tub1 and tub2) (fig. 2; $p = 0.0003$). Furthermore, the analysis according to the WHO classification also yielded a similar result.

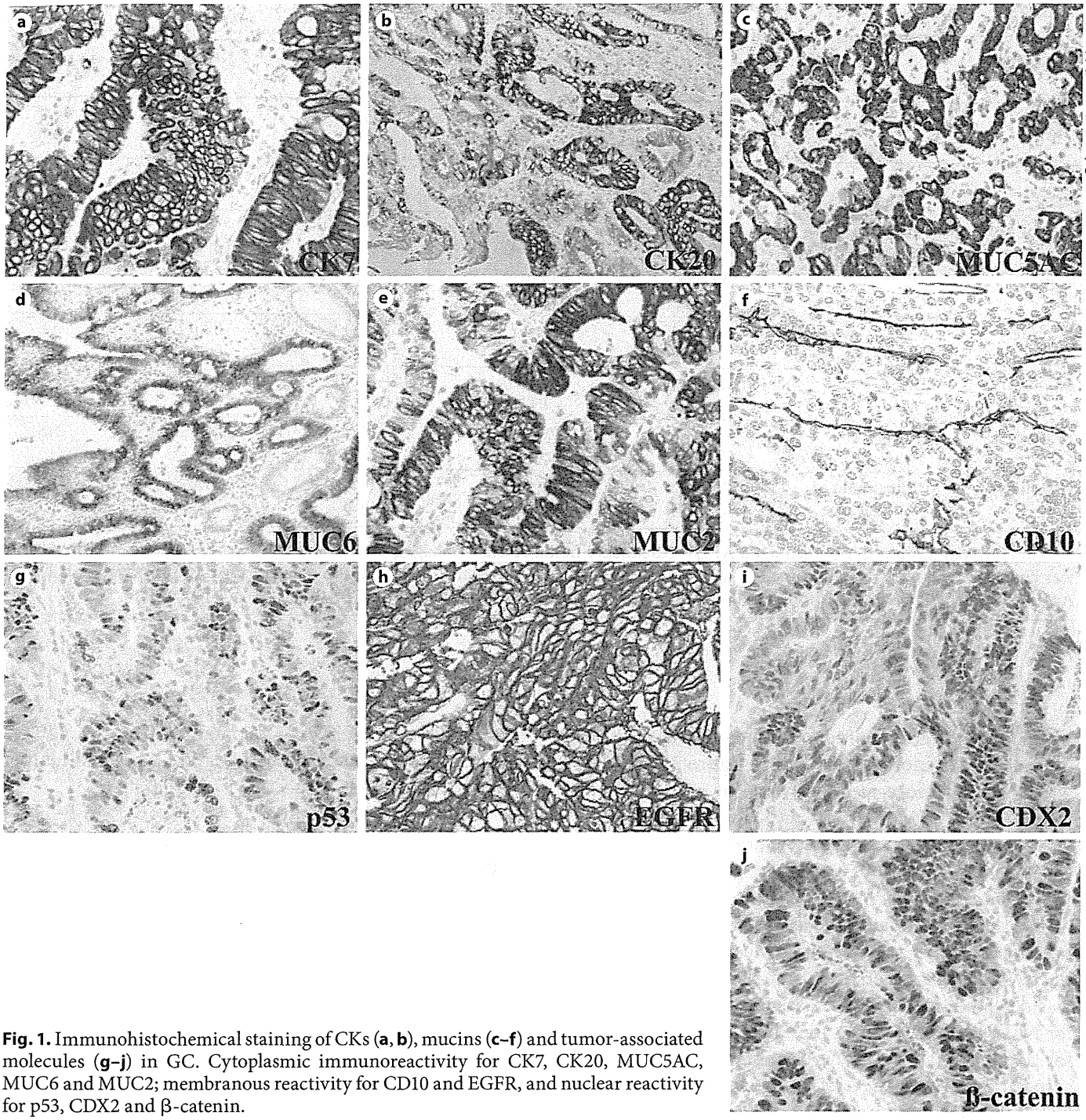

Fig. 1. Immunohistochemical staining of CKs (**a**, **b**), mucins (**c–f**) and tumor-associated molecules (**g–j**) in GC. Cytoplasmic immunoreactivity for CK7, CK20, MUC5AC, MUC6 and MUC2; membranous reactivity for CD10 and EGFR, and nuclear reactivity for p53, CDX2 and β-catenin.

Distribution of Mucin Phenotypes and Histological Types of GC

Next, we analyzed the relationships between the histological type and the mucin phenotype in the GCs. The 870 GCs included 519 (60%) cases with MUC5AC expression, 233 (27%) cases with MUC6 expression, 199 (23%) cases with MUC2 expression and 71 (8%) cases with CD10 expression. They were classified into 313 (36%) G type, 196 (23%) GI type, 149 (17%) I type and 212 (24%) N type. The distribution of each mucin phenotype and

Table 2. Relationships between CK expression patterns and clinicopathological findings in 870 GCs

CK pattern		CK7+/CK20+ (n = 156)	CK7+/CK20– (n = 492)	CK7–/CK20+ (n = 76)	CK7–/CK20– (n = 146)	p value
Age	>65 years	74 (47)	258 (52)	35 (46)	79 (54)	NS
	≤65 years	82 (53)	234 (48)	41 (54)	67 (46)	
Sex	Male	93 (60)	322 (65)	41 (54)	97 (66)	NS
	Female	63 (40)	170 (35)	35 (46)	49 (34)	
Tumor location	AEG	10 (6)	28 (6)	6 (8)	7 (5)	NS
	Distal GC	146 (94)	464 (94)	70 (92)	139 (95)	
T grade	T1	91 (58)	214 (43)	29 (38)	69 (47)	NS
	T2/T3/T4	65 (42)	278 (57)	47 (62)	77 (53)	
N grade	N0	107 (69)	279 (57)	36 (47)	82 (56)	NS
	N1	49 (31)	213 (43)	40 (53)	64 (44)	
M grade	M0	155 (99)	484 (98)	76 (100)	146 (100)	NS
	M1	1 (1)	8 (2)	0	0	
Staging	Stage I	106 (68)	277 (56)	36 (47)	81 (55)	NS
	Stage II/III/IV	50 (32)	215 (44)	40 (53)	65 (45)	
Histology	Intestinal type	105 (67)	285 (58)	52 (68)	61 (42)	0.0003
	Diffuse type	51 (33)	207 (42)	24 (32)	85 (58)	

Values in parentheses are percentages. AEG = Adenocarcinoma of the esophagogastric junction; NS = not significant. A $p < 0.001$ was considered statistically significant by χ^2 test. Tumor staging was classified according to the criteria of the International Union Against Cancer TNM classification of malignant tumors. Histology was according to the Lauren classification system.

histological type according to the Japanese Classification of Gastric Carcinomas is shown in figure 2. The N type was observed more frequently in the undifferentiated type GC.

Association of Expression between CK Patterns and Various Molecules

We then investigated the association between CK expression patterns and various molecules in the GCs. Of the 870 GCs examined, each tumor-associated molecule was detected in 293 (34%) cases for p53, 109 (13%) cases for EGFR, 183 (21%) cases for CDX2 and 140 (16%) cases for β-catenin (table 1). There are statistically significant associations between CK7 and MUC5AC expression, CK7 and MUC6 expression, CK20 and MUC2 expression, and CK20 and CDX2 ($p < 0.0001$) (fig. 3).

Association of CK Expression Patterns with Mucin Phenotypes

The relationship between each CK expression pattern and mucin phenotype in the 870 GCs was analyzed. As shown in figure 4, there are statistically significant associations between CK7 expression without CK20 expression and G type, CK7 expression and GI type, CK20 expression without CK7 expression and I type, and neither of them and N type, respectively ($p < 0.0001$).

Discussion

Much interest has focused on CK immunoprofiles in the classification of carcinomas, in particular the CK7 and CK20 profiles. There are many reports on the expression of CK7 and CK20 in relatively small numbers of GC cases [5, 6, 9, 12–21]. CK7 immunoreactivity is reported to range from 10 to 75%, while CK20 expression is frequently reported to range from 30 to 50%. Our results are also consistent with the findings of previous reports. The differences of positive rates in these previous reports are possibly due to evaluation scales and case groups. In this study, we used the TMA method to examine each molecule expression in the GCs. Although minute TMAs cannot ensure representative areas of donor specimen, we used 2-mm-diameter needles, which are large enough to evaluate the morphological appearance if representative regions are carefully selected with HE slides [25, 26]. In

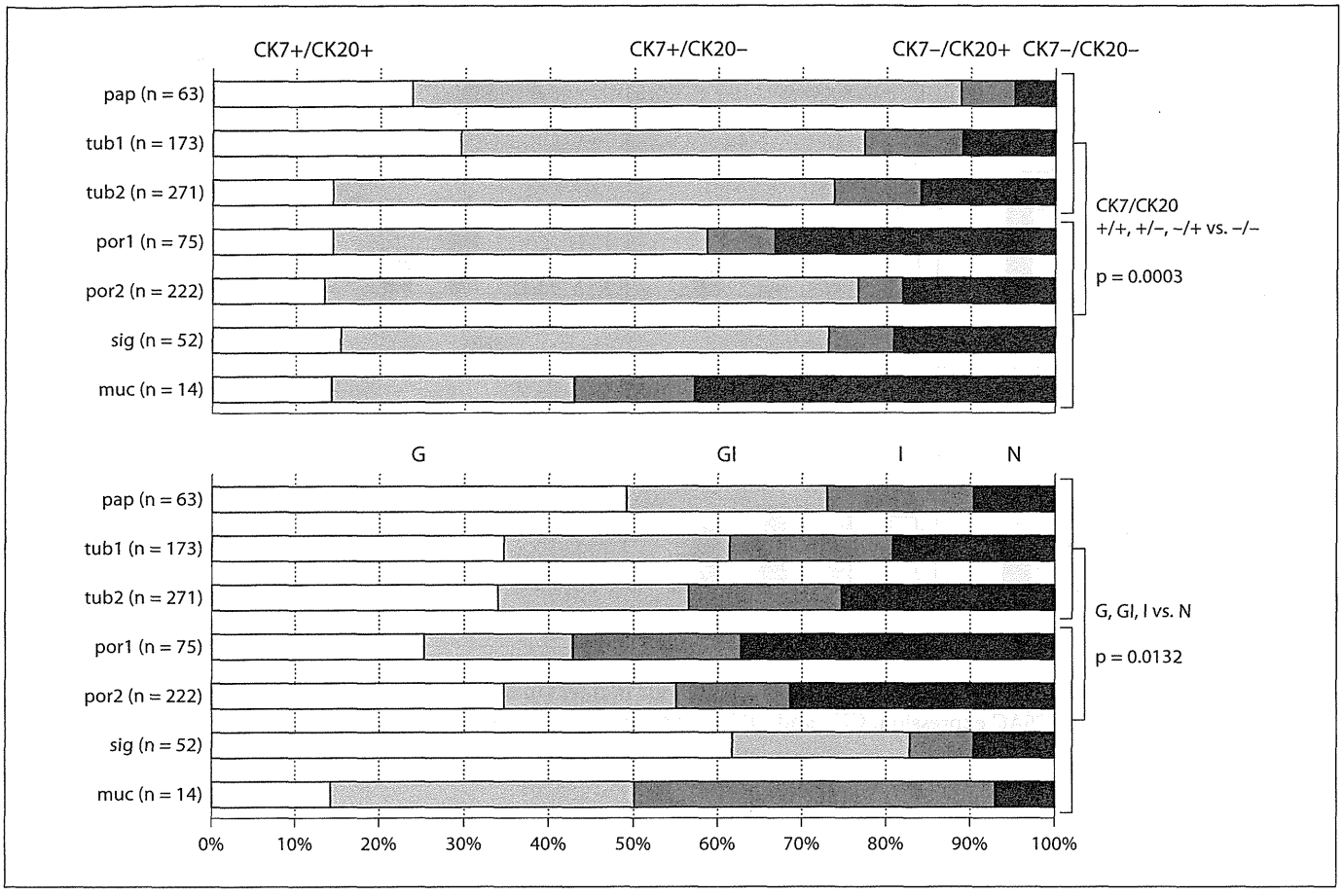

Fig. 2. The relationships between detailed histological type and CK expression patterns and mucin phenotypes in 870 GCs. The 870 GCs were histologically classified as 507 of the differentiated type (papillary adenocarcinoma or tubular adenocarcinoma) and 363 of the undifferentiated type (poorly differentiated adenocarcinoma, signet-ring cell carcinoma or mucinous adenocarcinoma). There are statistically significant associations between the undifferentiated type and neither CK7 nor CK20 expression, and the undifferentiated type and N mucin phenotype.

terms of the possible diversity of histological components or molecular abnormality in the GCs, several previous reports have shown an excellent concordance between the results obtained from TMAs and those from full sections [27, 28]. Furthermore, the effects of intratumoral heterogeneity can be averaged out in such a large-scale analysis as the present study. It is unlikely that the use of TMA biased the outcome.

To clarify the significance of the CK expression patterns, we analyzed the relation between CK expression patterns and the clinicopathologic parameters, histology, mucin phenotype or several tumor-related molecules. Histologically, expression of CK7 and/or CK20 showed a tendency toward a high positive rate in differentiated type GC and a low positive rate in undifferentiated type GC. This may reflect a loss of the ability to produce the CKs along with a decrease in histological differentiation in neoplastic cells. However, CK7 and/or CK20 expression was not associated with any other clinicopathologic features, consistent with the previous report [17, 29]. GCs have been classified into four mucin phenotypes. Previous reports provided evidence that mucin expression is closely associated with the differentiation of GCs [30, 31]. In the present study, G type was correlated with CK7 expression, especially in the absence of CK20 expression, whereas I type was correlated with CK20 expression, especially in the absence of CK7 expression. This result demonstrated statistical significance, but neither CK7 nor CK20 was sufficient for the discrimination of the mucin phenotype due to low sensitivity and specificity. In the present study,

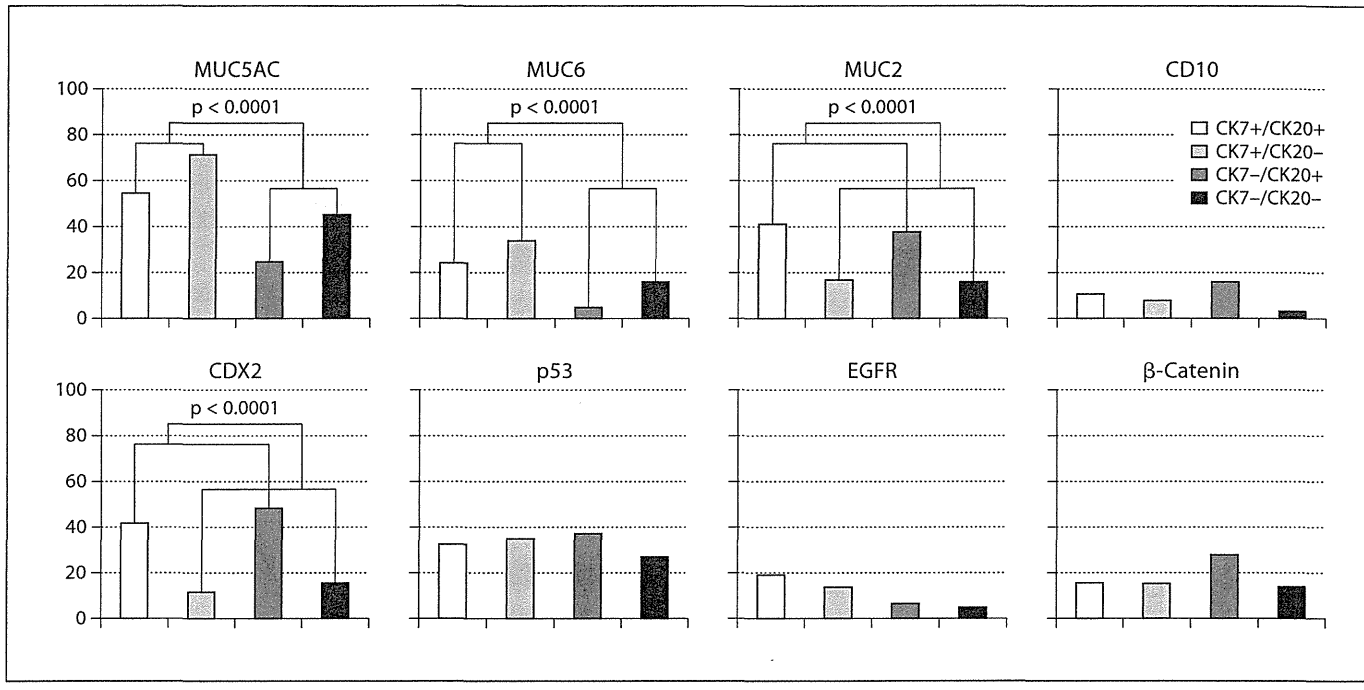

Fig. 3. The relationships between CK expression patterns and various markers in 870 GCs. There are statistically significant associations between CK7 and MUC5AC expression, CK7 and MUC6 expression, CK20 and MUC2 expression, and CK20 and CDX2 ($p < 0.0001$).

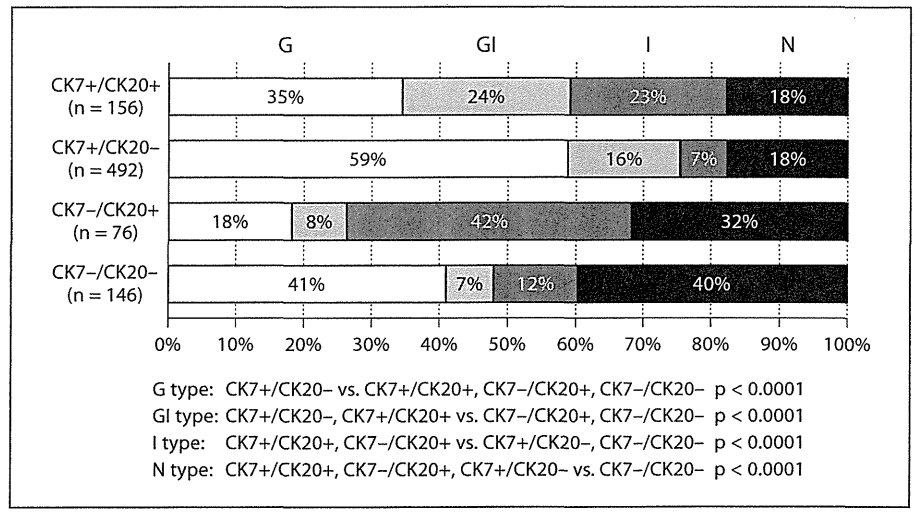

Fig. 4. The relationships between each CK expression pattern and mucin phenotypes in 870 GCs. There are statistically significant associations between CK7 expression without CK20 expression and G mucin phenotype, CK7 expression and GI mucin phenotype, CK20 expression without CK7 expression and I mucin phenotype, and neither of them and N mucin phenotype ($p < 0.0001$).

the positive expression of CK20 was frequently observed in GCs with the I type and showed significant correlation with the positive expression of Cdx2. There is no previous report showing a direct association between CK20 and Cdx2. Chan et al. [32] reported that CK20 is directly regulated by Cdx1. Therefore, there may also be a close correlation between CK20 and CDX2.

In summary, GCs showed heterogenous CK expression representing their histological features. Therefore, a single CK and its combination does not always provide diagnostic value in differentiating GCs. Advances in our understanding of the genetic and molecular bases of GC according to each CK expression, however, may lead to new therapy.

Acknowledgements

We thank Ms. Emiko Hisamoto and Mr. Shinichi Norimura for their excellent technical assistance and advice. This work was carried out with the kind cooperation of the Research Center for Molecular Medicine, Faculty of Medicine, Hiroshima University. We also thank the Analysis Center of Life Science, Hiroshima University, for the use of its facilities. This work was supported in part by Grants-in-Aid for Cancer Research from the Ministry of Education, Culture, Science, Sports and Technology of Japan and in part by a Grant-in-Aid for the Third Comprehensive 10-Year Strategy for Cancer Control and for Cancer Research from the Ministry of Health, Labour and Welfare of Japan.

References

1 Carneiro F, Sobrinho-Simoes M: Metastatic pattern of gastric carcinoma. Hum Pathol 1996;27:213–214.
2 Yasui W, Oue N, Kitadai Y, Nakayama H: Recent advances in molecular pathobiology of gastric carcinoma; in Kaminishi M, Takubo K, Mafune K (eds): The Diversity of Gastric Carcinoma: Pathogenesis, Diagnosis and Therapy. Tokyo, Springer, 2005, pp 51–71.
3 Tatematsu M, Tsukamoto T, Inada K: Stem cells and gastric cancer: role of gastric and intestinal mixed intestinal metaplasia. Cancer Sci 2003;94:135–141.
4 Yasui W, Sentani K, Motoshita J, Nakayama H: Molecular pathobiology of gastric cancer. Scand J Surg 2006;95:225–231.
5 Chu PG, Weiss LM: Keratin expression in human tissues and neoplasms. Histopathology 2002;40:403–439.
6 Chu P, Wu E, Weiss LM: Cytokeratin 7 and cytokeratin 20 expression in epithelial neoplasms: a survey of 435 cases. Mod Pathol 2000;13:962–972.
7 Moll R: Cytokeratins in the histological diagnosis of malignant tumors. Int J Biol Markers 1994;9:63–69.
8 Moll R, Lowe A, Laufer J, Franke WW: Cytokeratin 20 in human carcinomas. A new histodiagnostic marker detected by monoclonal antibodies. Am J Pathol 1992;140:427–447.
9 Schwerer MJ, Baczako K: Expression of cytokeratins typical for ductal and squamous differentiation in the human stomach: an immunohistochemical study of normal foveolar epithelium, *Helicobacter pylori* gastritis and intestinal metaplasia. Histopathology 1996;29:131–137.
10 Ramaekers F, van Niekerk C, Poels L, Schaafsma E, Huijsmans A, Robben H, Schaart G, Vooijs P: Use of monoclonal antibodies to keratin 7 in the differential diagnosis of adenocarcinomas. Am J Pathol 1990; 136:641–655.
11 Tot T: Cytokeratins 20 and 7 as biomarkers: usefulness in discriminating primary from metastatic adenocarcinoma. Eur J Cancer 2002;38:758–763.
12 Park SY, Kim HS, Hong EK, Kim WH: Expression of cytokeratins 7 and 20 in primary carcinomas of the stomach and colorectum and their value in the differential diagnosis of metastatic carcinomas to the ovary. Hum Pathol 2002;33:1078–1085.
13 Moll R: Cytokeratins as markers of differentiation in the diagnosis of epithelial tumors. Subcell Biochem 1998;31:205–262.
14 Wauters CC, Smedts F, Gerrits LG, Bosman FT, Ramaekers FC: Keratins 7 and 20 as diagnostic markers of carcinomas metastatic to the ovary. Hum Pathol 1995;26:852–855.
15 Kirchner T, Muller S, Hattori T, Mukaisyo K, Papadopoulos T, Brabletz T, Jung A: Metaplasia, intraepithelial neoplasia and early cancer of the stomach are related to dedifferentiated epithelial cells defined by cytokeratin-7 expression in gastritis. Virchows Arch 2001;439:512–522.
16 Ormsby AH, Goldblum JR, Rice TW, Richter JE, Gramlich TL: The utility of cytokeratin subsets in distinguishing Barrett's-related oesophageal adenocarcinoma from gastric adenocarcinoma. Histopathology 2001;38: 307–311.
17 Kim MA, Lee HS, Yang HK, Kim WH: Cytokeratin expression profile in gastric carcinomas. Hum Pathol 2004;35:576–581.
18 Shen B, Ormsby AH, Shen C, Dumot JA, Shao YW, Bevins CL, Gramlich TL: Cytokeratin expression patterns in noncardia, intestinal metaplasia-associated gastric adenocarcinoma: implication for the evaluation of intestinal metaplasia and tumors at the esophagogastric junction. Cancer 2002;94: 820–831.
19 Gurbuz Y, Kose N: Cytokeratin expression patterns of gastric carcinomas according to Lauren and Goseki classification. Appl Immunohistochem Mol Morphol 2006;14:303–308.
20 Lee MJ, Lee HS, Kim WH, Choi Y, Yang M: Expression of mucins and cytokeratins in primary carcinomas of the digestive system. Mod Pathol 2003;16:403–410.
21 Xue L, Zhang X, Li Y, Yang H, Li X, Mi J, Wang H, Wang J, Yan X: Differences of immunophenotypic markers and signaling molecules between adenocarcinomas of gastric cardia and distal stomach. Hum Pathol 2011;42:594–601.
22 Sobin LH, Wittekind CH (eds): TNM Classification Of Malignant Tumors, ed 6. New York, Wiley, 2002, pp 65–68.
23 Japanese Gastric Cancer Association: Japanese classification of gastric carcinoma, 3rd English edition. Gastric Cancer 2011;14:101–112.
24 Mizoshita T, Tsukamoto T, Nakanishi H, Inada K, Ogasawara N, Joh T, Itoh M, Yamamura Y, Tatematsu M: Expression of Cdx2 and the phenotype of advanced gastric cancers: relationship with prognosis. J Cancer Res Clin Oncol 2003;129:727–734.
25 Sauter G, Mirlacher M: Tissue microarrays for predictive molecular pathology. J Clin Pathol 2002;55:575–576.
26 Sentani K, Oue N, Tashiro T, Sakamoto N, Nishisaka T, Fukuhara T, Taniyama K, Matsuura H, Arihiro K, Ochiai A, Yasui W: Immunohistochemical staining of reg IV and claudin-18 is useful in the diagnosis of gastrointestinal signet ring cell carcinoma. Am J Surg Pathol 2008;32:1182–1189.
27 Hoos A, Urist MJ, Stojadinovic A, Mastorides S, Dudas ME, Leung DH, Kuo D, Brennan MF, Lewis JJ, Cordon-Cardo C: Validation of tissue microarrays for immunohistochemical profiling of cancer specimens using the example of human fibroblastic tumors. Am J Pathol 2001;158:1245–1151.
28 Lee HS, Cho SB, Lee HE, Kim MA, Kim JH, Park do J, Kim JH, Yang HK, Lee BL, Kim WH: Protein expression profiling and molecular classification of gastric cancer by the tissue array method. Clin Cancer Res 2007; 13:4154–4163.
29 Gulmann C, Counihan I, Grace A, Patchett S, Leen E, Leader M, Kay E: Cytokeratin 7/20 and mucin expression patterns in oesophageal, cardia and distal gastric adenocarcinomas. Histopathology 2003;43:453–461.
30 Pinto-de-Sousa J, David L, Reis CA, Gomes R, Silva L, Pimenta A: Mucins MUC1, MUC2, MUC5AC and MUC6 expression in the evaluation of differentiation and clinicobiological behaviour of gastric carcinoma. Virchows Arch 2002;440:304–310.
31 Pinto-de-Sousa J, Reis CA, David L, Pimenta A, Cardoso-de-Oliveira M: MUC5B expression in gastric carcinoma: relationship with clinico-pathological parameters and with expression of mucins MUC1, MUC2, MUC5AC and MUC6. Virchows Arch 2004;444: 224–230.
32 Chan CW, Wong NA, Liu Y, Bicknell D, Turley H, Hollins L, Miller CJ, Wilding JL, Bodmer WF: Gastrointestinal differentiation marker cytokeratin 20 is regulated by homeobox gene CDX1. Proc Natl Acad Sci USA 2009;106:1936–1941.

Pathology International

Pathology International 2012; **62**: 112–119 doi:10.1111/j.1440-1827.2011.02760.x

Original Article

Expression of cancer stem cell markers ALDH1, CD44 and CD133 in primary tumor and lymph node metastasis of gastric cancer

Yuta Wakamatsu, Naoya Sakamoto, Htoo Zarni Oo, Yutaka Naito, Naohiro Uraoka, Katsuhiro Anami, Kazuhiro Sentani, Naohide Oue and Wataru Yasui

Department of Molecular Pathology, Hiroshima University Graduate School of Biomedical Sciences, Hiroshima, Japan

Gastric cancer (GC) is one of the most common malignancies worldwide. Recently, cancer stem cells (CSCs) in tumors were found to possess the ability to sustain tumor self-renewal, initiate tumor progression, and possibly also contribute to cancer metastasis. We immunohistochemically examined expression and distribution of representative CSC markers ALDH1, CD44, and CD133 in primary tumors and lymph node metastasis of GC. Among 190 GC primary tumors, 104 (55%) were positive for ALDH1, 117 (62%) were positive for CD44, and 18 (9%) were positive for CD133. Expression of these three CSC markers was significantly associated with advanced clinicopathologic factors. Patients with CD44- and CD133-positive GC had a poorer survival rate than patients with CD44- and CD133-negative GC (CD44: $P < 0.001$, CD133: $P = 0.006$). Univariate and multivariate Cox proportional hazards analysis revealed tumor node metastasis stage, CD44 expression, and CD133 expression to be independent predictors of survival in patients with GC. Comparison of CSC markers in primary and metastatic sites showed ALDH1 positivity to be significantly higher in diffuse-type lymph node metastasis than in the primary tumor ($P < 0.001$). These results indicate that these CSC markers are important in tumor invasion and metastasis and may be good markers indicating long-term survival in patients with GC.

Key words: cancer stem cell, gastric cancer, metastasis, stem cell marker

Correspondence: Wataru Yasui, MD, PhD, Department of Molecular Pathology, Hiroshima University Graduate School of Biomedical Sciences, 1-2-3 Kasumi, Minami-ku, Hiroshima 734-8551, Japan. E-mail: wyasui@hiroshima-u.ac.jp

Received 25 July 2011. Accepted for publication 6 October 2011.

Gastric cancer (GC) is one of the most common human cancers. According to the World Health Organization, GC is the fourth most common malignancy worldwide, with approximately 870 000 new cases occurring yearly.[1] Cancer develops as a result of multiple genetic and epigenetic alterations. Cancer at an advanced stage is a systemic disease and metastatic status significantly affects patient outcomes. In GC, lymph node metastasis is one of the most valuable prognostic factors. It is an important issue to examine the biological characteristics of cancer cells not only in primary tumors but also in metastatic tumors in the lymph node. However, the molecular pathological features of metastatic sites have not been sufficiently analyzed.

Recently, the cancer stem cell model suggests that in many cancers, tumor initiation and propagation is driven by a population of self-renewing tumor cells known as cancer stem cells (CSCs).[2] CSCs also promote tumor cell heterogeneity, metastasis, and therapeutic resistance, and are potentially driven by known oncogenic signaling pathways.[3,4] The study of CSCs would be greatly enhanced by the availability of specific markers to identify and isolate these cells. Through examinations using putative stem cell markers or side population (SP), unique subsets of cancer cells from different types of tumors have been detected. These markers include CD133, CD44, CD24, and CD166. Among them, both CD133 and CD44 are widely used for isolating CSCs from solid tumors. CD133 is a cell surface transmembrane glycoprotein, which exists in the cholesterol-rich domain of lipid rafts, and was identified in subpopulations of cells in brain and colon tumors.[5,6] Only one hundred CD133-positive cells implanted in a non-obese diabetic severe combined immunodeficient (NOD-SCID) mouse are sufficient to initiate a tumor, and isolated stem cells from this tumor can be serially passed to other NOD-SCID mice.[5,7] Expression of CD133 has been reported to be associated with poor prognosis in

GC.[8,9] CD44 is also a transmembrane glycoprotein which participates in many cellular processes, including growth, survival, differentiation, and mortality,[10,11] and plays important roles in malignant behaviors of several human cancers including GC.[12–14] The CD44 marker can be used to isolate CSC populations of prostate,[15] pancreas,[16] and colorectal tumors.[17] Recent reports indicate that CD44-positive fractions of GC can generate spheroid colonies under non-adherent conditions and that small numbers of these cells can generate tumors in SCID mice.[18]

Beside these markers, a promising new marker for CSC is aldehyde dehydrogenase 1 (ALDH1).[19,20] Aldehyde dehydrogenase enzymes are a family of intracellular enzymes that participate in cellular detoxification, differentiation, and drug resistance through the oxidation of cellular aldehydes.[21] ALDH1 positive cells monitored by immunohistochemistry and flow cytometry occupy a considerably smaller subpopulation that is about one-seventh of the size of the CD44- and CD133-positive populations. Nevertheless, ALDH1-positive cell populations are capable of generating tumor xenografts.[20] Therefore, ALDH1 may be able to label a cell population closely related to stem cells. Moreover, high percentages of ALDH1-positive cells in most types of epithelial tumors are associated with poorer clinical outcomes for these patients.[19,22,23] However, expression of ALDH1 in GC has not been analyzed.

In this present study, we examined the expression and distribution of the representative CSC markers ALDH1, CD44 and CD133 in GC by immunohistochemistry, and studied their relationship with clinicopathologic features. Furthermore, the expression of CSC markers was compared between GC primary tumors and metastatic lymph nodes.

MATERIALS AND METHODS

Tissue samples

In total, 190 primary tumor samples were collected from patients diagnosed with GC. Patients were treated at the Hiroshima University Hospital or affiliated hospitals. Of the 190 GC samples, associated lymph node metastasis samples were available for 104 cases. Information on patient prognosis was available for 96 of the 190 GC cases. Because written informed consent was not obtained, for strict privacy protection, identifying information for all samples was removed before analysis. This procedure was in accordance with the Ethical Guidelines for Human Genome/Gene Research of the Japanese Government.

For immunohistochemical analysis, we used formalin-fixed, paraffin-embedded tissues from 190 patients who had undergone surgical excision for GC. One or two representative tumor blocks were examined from each patient by immunohistochemistry. Tumor staging was made according to the TNM classification system. Histological classification of GC was carried out according to the Lauren classification system; GC cases were classified into intestinal-, diffuse-, and mixed-type.

Immunohistochemical examination

Immunohistochemical staining was carried out according to the procedure previously reported.[24] Deparaffinized sections were deparaffinized in xylene, dehydrated in a graded ethanol series, and immersed in a 0.3% hydrogen peroxide solution in methanol for 10 min to inhibit endogenous peroxidase activity. The sections were placed in ethylenediaminetetraacetic acid buffer at pH 8.0 for CD133, or citrate buffer (pH 6.0) for ALDH1 and CD44 stainings. For antigen retrieval, the slides were heated at 95°C for 20 min in a microwave oven for CD133, or 95°C for 30 min in a microwave oven for ALDH1 and CD44 staining, and allowed to cool for 5 min at room temperature. Sections were incubated with the following antibody dilutions; primary anti-CD133 antibody (AC133; Miltenyi Biotec, Auburn, CA, USA) 1:100, anti-ALDH1 antibody (BD Biosciences; San Diego, CA, USA) 1:200, and anti-CD44 antibody (Novocastra; Newcastle, UK). Sections were incubated with primary antibody for 1 h at room temperature. The slides were washed three times with PBS, followed by incubations with Envision+ anti-mouse peroxidase for 1 h. For color reactions, sections were incubated with the DAB Substrate-Chromogen Solution (Dako Cytomation; Carpinteria, CA, USA) for 10 min. Sections were then counterstained with 0.1% hematoxylin. Previous reports demonstrated that significant correlation between poor clinical outcome and immunostaining with CD133 in colorectal cancer,[25] CD44 in squamous cell carcinoma of lung,[26] and ALDH1 in non-small cell carcinoma of lung.[27] According to the definition of positive staining in these previous reports, the result was considered positive if at least 10% of the cells were stained. When fewer than 10% of cancer cells were stained, the immunostaining was considered negative.

Statistical analysis

ALDH1, CD44, and CD133 expression and clinicopathologic features were tested for association by the χ^2 test. For each molecule, Kaplan–Meier survival curves were constructed to compare positive and negative patients. Differences between survival curves were tested for statistical significance by log-rank test. Univariate and multivariate Cox regression was used to evaluate the associations between clinical covariates and cancer-specific mortality in SPSS (SPSS Inc., Chicago, IL, USA). Hazard ratio (HR) and 95% confidence interval (CI)

Table 1 Association of cancer stem cell (CSC) marker staining with clinicopathologic features of gastric cancer (GC)

	ALDH1		CD44		CD133	
Total	104/190 (55%)		117/190 (62%)		18/190 (9%)	
% positive cells in stained case	10–90%		10–90%		10–40%	
Characters	Positive rate	*P*-value*	Positive rate	*P*-value*	Positive rate	*P*-value*
T grade†						
T1	19/45 (42%)	0.02	25/45 (56%)	0.36	4/45 (9%)	0.92
T2/3/4	85/145 (58%)		92/145 (63%)		14/145 (9%)	
N grade†						
N0	49/80 (61%)	0.14	42/80 (53%)	0.04	3/80 (4%)	0.02
N1/2/3	55/110 (50%)		75/110 (68%)		15/110 (14%)	
TNM stage†						
Stage I/II	29/69 (42%)	0.01	32/69 (46%)	<0.001	4/69 (5%)	0.24
Stage III/IV	75/121 (61%)		85/121 (70%)		14/121 (11%)	
Histology‡						
Intestinal	57/72 (79%)	<0.001§	47/72 (47%)	0.43§	13/72 (18%)	<0.001§
Diffuse	37/94 (39%)		57/94 (60%)		4/94 (4%)	
Mixed	10/24 (41%)		13/24 (54%)		1/24 (4%)	

*χ^2 test: $P < 0.05$ was considered significant.

†Tumor stage was classified according to the criteria of the International Union Against Cancer Tumor Node Metastasis (TNM) classification of malignant tumors.

‡Histology was according to the Lauren classification.

§Intestinal versus Diffuse plus Mixed-type.

ALDH1, aldehyde dehydrogenase 1.

were estimated from Cox proportional hazard models. For all analyses, age was treated as a categorical variable (65 years old plus, more than 65 years old, versus less than 65 years old). For final multivariable Cox regression models, all variables were included that were moderately associated with cancer-specific mortality ($P < 0.10$). All *P*-values were two-sided, and the significance level was set at $P < 0.05$.

RESULTS

Expression of CSC markers (ALDH1, CD44, CD133) in non-neoplastic gastric mucosa and GC

We examined the expression of ALDH1, CD44, and CD133 by immunohistochemical staining in normal gastric mucosa, intestinal metaplasia, and a series of 190 specimens of GC. In normal gastric mucosa, staining of ALDH1 was detected in the cytoplasm of parietal cells. CD44 was detected in lymphocytes and stromal cells but not epithelial cells; this is consistent with a previous report.[28] CD133 staining was not detected in normal gastric epithelial and stromal cells. Although stem cells of normal gastric gland are considered to be located in the gastric isthmus; no staining of these three molecules was observed in this region. In intestinal metaplasia, CD44 and ALDH1 expression were found in the basal lesion of the metaplastic gland (data not shown). This expression pattern mimics that of the normal colon as per previous reports.[20,29] CD133 staining was not detected in metaplastic lesions.

Out of 190 cases of GC, 104 (55%) were positive for ALDH1, 117 (62%) were positive for CD44, and 18 (9%) were positive for CD133 (Table 1). ALDH1 and CD44 were also observed mainly in the cytoplasm and the membrane of the tumor cells, respectively. Many tumor cells were positive for ALDH1 and CD44 in both intestinal-type and diffuse-type GC (Fig. 1a, b, d and e). CD133 was expressed in the apical membrane of the tumor cells. CD133-positive staining was observed in intestinal-type and diffuse-type GC with partial glandular formation (Fig. 1c,f). In GC, the percentage of ALDH1- and CD44-stained tumor cells ranged from 0% to 90%, and the percentage of CD133-stained tumor cells ranged from 0% to 40% (Table 1). More than half of ALDH1- and CD44-positive cases contained over 50% positive cancer cells. CD44 expression was detected in whole tumor lesions. Most CD133-positive cases included less than 20% positive cancer cells. For each CSC marker, immunostaining was considered positive when at least 10% of tumor cells were stained, on the basis of previous reports.[25–27]

Correlation between CSC markers and clinicopathologic features

The relationship of CSC marker staining to clinicopathologic characteristics was investigated (Table 1). ALDH1-positive GC cases showed more advanced T stage ($P = 0.02$, χ^2 test), TNM stage ($P = 0.01$, χ^2 test), and tended to be intestinal histology ($P < 0.001$, χ^2 test) than ALDH1-negative cases. CD44-positive GC cases showed more advanced N stage

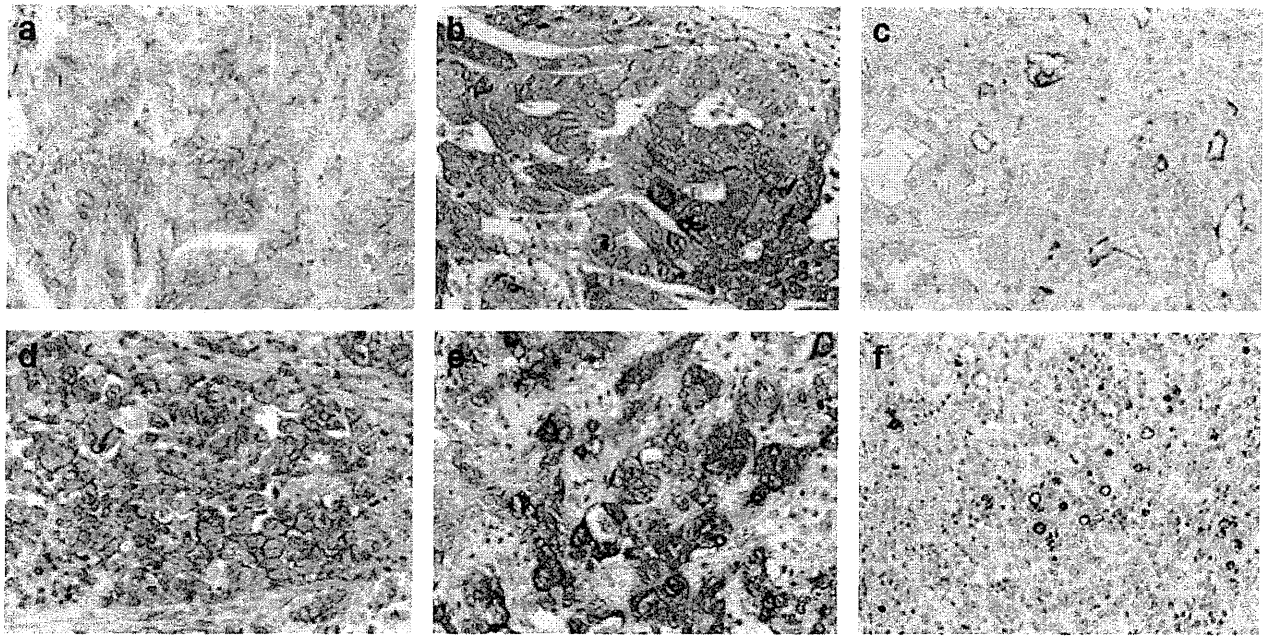

Figure 1 Immunohistochemical analysis of cancer stem cell (CSC) makers in gastric cancer (GC) tissue. Membranous staining of CD44 was observed in intestinal-type (a) and diffuse-type (d) GC (Original magnification: ×400). cytoplasmic staining of aldehyde dehydrogenase 1 (ALDH1) was observed in intestinal-type (b) and diffuse-type (e) GC (Original magnification: ×400). Staining of CD133 was observed in apical membranes in intestinal-type GC (c) and diffuse-type GC with partial glandular formation (f) (Original magnification: ×400).

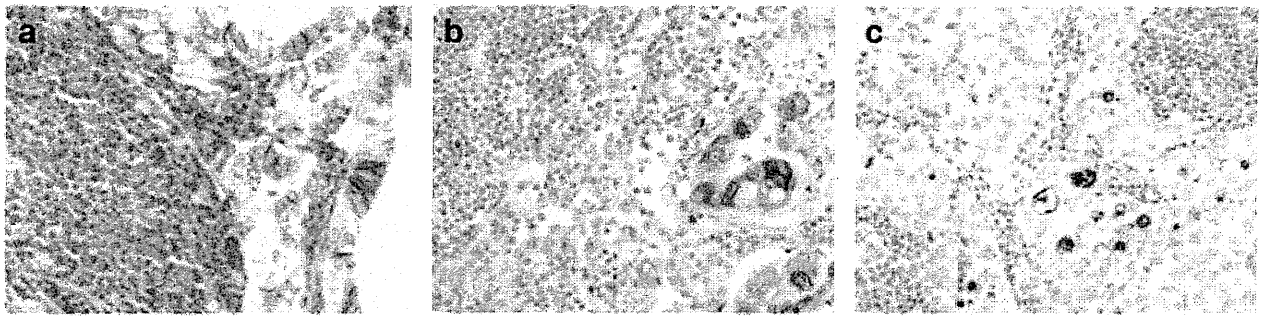

Figure 3 Immunohistochemical analysis of cancer stem cell (CSC) markers in lymph node metastasis of gastric cancer (GC). Expression pattern of CD44 (a), aldehyde dehydrogenase 1 (ALDH1) (b), and CD133 (c) in GC lymph node metastasis of (Original magnification: ×400). The staining patterns of all molecules were similar to those of the primary site.

($P = 0.04$, χ^2 test) and TNM stage ($P < 0.001$, χ^2 test) than CD44-negative cases. CD133-positive GC cases also showed more advanced N stage ($P = 0.02$, χ^2 test) and tended to be intestinal-type in histological character ($P = 0.03$, χ^2 test).

Correlation between 5 year overall survival and the CSC marker expression

The relationship between survival probability and CSC marker staining was examined in 96 GC cases. The 5 year overall survival rate was 48% for CD44-positive cases and 62% for CD44-negative cases. The 5 year overall survival rate was 35% for ALDH1-positive cases and 46% for ALDH1-negative cases. For CD133, the 5 year overall survival rate was 0% for positive cases and 52% negative cases. CD44-positive patients had significantly lower survival probability than CD44-negative patients ($P < 0.001$; Fig. 2a). Moreover, CD133-positive cases had a shorter overall survival time than CD133-negative cases ($P = 0.006$; Fig. 2b), whereas staining with ALDH1 had no prognostic impact ($P = 0.94$; Fig. 2c). We also investigated the relationship between survival probability and CSC marker staining in 59 cases of advanced GC (more

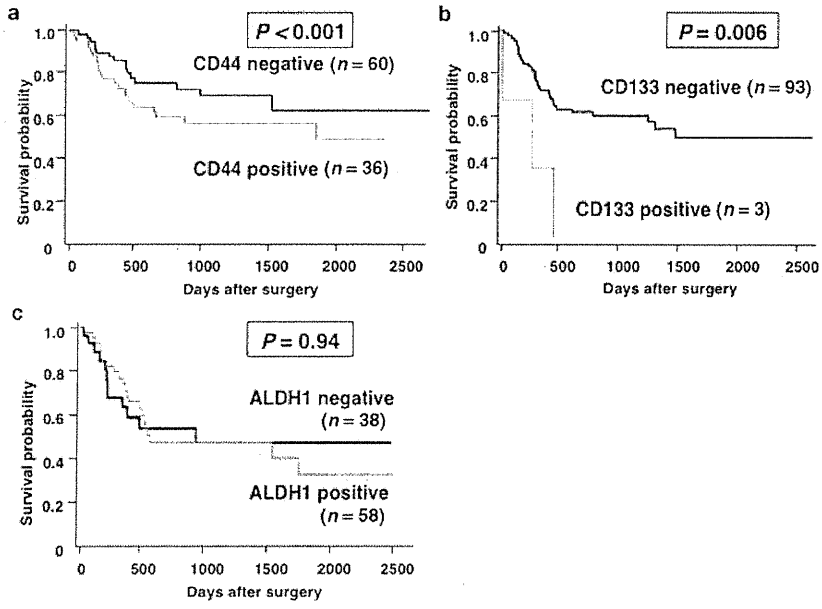

Figure 2 Survival of patients with gastric cancer (GC). (a) Kaplan–Meier curves of patients with CD44-negative or CD44-positive GC. (b) Kaplan–Meier curves of patients with CD133-negative or CD133-positive GC. (c) Kaplan–Meier curves of patients with aldehyde dehydrogenase 1 (ALDH1)- negative or ALDH1-positive GC.

than stage II) and 38 cases of stage II and III, and obtained comparable results were obtained (advanced cases; CD133: $P < 0.001$, CD44: $P = 0.02$, ALDH1: $P = 0.56$, stage II and III cases; CD133: $P < 0.001$, CD44: $P = 0.006$, ALDH1: $P = 0.27$, log-rank test). In addition, because it is well-known that tumors displaying different histological types are associated with distinct biological behavior, we examined the relationship between survival and CSC marker staining in 42 cases of intestinal-type GC and 45 cases of diffuse-type GC, respectively. CD44 positivity significantly correlated with poor prognosis both in intestinal- and diffuse-type GC cases (intestinal-type: $P < 0.001$, diffuse-type: $P = 0.01$, log-rank test). CD133 positivity significantly correlated with poor prognosis in intestinal-type GC cases ($P = 0.004$, log-rank test). ALDH1 positivity had no prognostic impact in both histologic types (intestinal-type: $P = 0.93$, diffuse-type: $P = 0.91$, log-rank test).

To evaluate the potential for CSC markers as a prognostic classifier, the association of CSC markers expression with cancer-specific mortality was evaluated with both univariate and multivariate Cox proportional hazards analyses (Table 2). By univariate analysis, the TNM stage (HR, 6.37; 95% CI, 2.38–16.67; $P = 0.002$), CD44 expression (HR, 4.20; 95% CI, 1.92–9.09; $P < 0.001$), and CD133 expression (HR, 4.67; 95% CI, 1.08–20.00; $P = 0.04$) were associated with survival. By multivariate modeling, both CD44 expression (HR, 2.77; 95% CI, 1.19–6.25; $P = 0.02$) and CD133 expression (HR, 20.41; 95% CI, 3.70–100.00; $P < 0.001$) were independent prognostic indicators (Table 2). These results indicate that immunohistochemical examination of CD44 and CD133 in GC samples have potential as prognostic biomarkers for GC.

Comparison of CSC marker expression between primary and lymph node metastatic sites

Immunostaining of lymph node metastatic sites was performed. Compared with the positive rate and staining pattern of CSC markers in primary tumors, concordance rates were calculated as a combination of both positive and negative cases in primary and metastasis, divided by the total number of cases. Concordance rates of all CSC markers were more than 70% (Table 3). CSC markers expression pattern in lymph node metastasis tended to be the same as primary tumor (Fig. 3). Interestingly, when tumors were classified as intestinal-, diffuse- and mixed-types based on their Lauren classification, the positivity of ALDH1 in lymph node metastasis of the diffuse-type was significantly higher than that of the primary tumor ($P < 0.001$, χ^2 test, Table 4).

DISCUSSION

According to the CSC hypothesis, it is assumed that CSCs are responsible for cancer initiation and development. Expression of CSC markers have been reported to be present in normal adult stem/ progenitor cells as well as in CSC.[30,31] In this present study, we examined the expression and distribution of representative CSC markers (ALDH1, CD44 and CD133) in normal, metaplastic, and cancerous tissue of the stomach. Although we could not detect CSC marker staining in gastric pit, positive staining of CD44 and ALDH1 was detected at the crypt bottom of intestinal metaplasias, whose staining patterns closely resembled those of

Table 2 Univariate and multivariate Cox regression analysis of cancer stem cell (CSC) marker expression levels and overall survival (stage I-IV, $n = 65$)

Characteristic	Univariate analysis HR (95% CI)	*P*-value*	Multivariate analysis HR (95% CI)	*P*-value*
Age				
< 65	1 (Ref.)	0.41		
65 and 65<	1.38 (0.65–2.94)			
Sex				
Male	1 (Ref.)	0.40		
Female	0.72 (0.33–1.57)			
TNM stage†				
Stage I/II	1 (Ref.)	0.002	1 (Ref.)	0.002
Stage III/IV	6.37 (2.38–16.67)		6.41 (2.04–20.00)	
ALDH1 expression				
Negative	1 (Ref.)	0.40		
Positive	1.41 (0.32–1.57)			
Histology				
Intestinal	1	0.38		
Diffuse and mixed	1.27 (0.56–2.43)			
Histology				
Intestinal and mixed	1	0.21		
Diffuse	0.86 (0.24–1.22)			
CD44 expression				
Negative	1 (Ref.)	<0.001	1 (Ref.)	0.02
Positive	4.20 (1.92–9.09)		2.77 (1.19–6.25)	
CD133 expression				
Negative	1 (Ref.)	0.04	1 (Ref.)	<0.001
Positive	4.67 (1.09–20.00)		20.41 (3.70–100.00)	

*χ^2 test: $P < 0.05$ was considered significant.

†Tumor stage was classified according to the criteria of the International Union Against Cancer Tumor Node Metastasis (TNM) classification of malignant tumors.

ALDH1, aldehyde dehydrogenase 1; CI, confidence interval; HR, hazard ratio.

Table 3 Positive rate and concordance rate of cancer stem cell (CSC) marker expression in primary gastric cancer (GC) and metastasis

Total	Positive rate	Concordance rate†
ALDH1		
Primary	60/104 (57%)	73/104 (70%)
Metastasis	77/104 (74%)	
CD44		
Primary	60/104 (57%)	78/104 (75%)
Metastasis	62/104 (59%)	
CD133		
Primary	14/104 (13%)	91/104 (87%)
Metastasis	9/104 (8%)	

†Concordance rate; calculated as a combination of both positive and negative cases in primary and metastasis, divided by total number of cases.

ALDH1, aldehyde dehydrogenase 1.

the normal colon.[20,26] Taken together, immunohistochemical analysis of these markers are not useful for detecting normal stem cells of the stomach. In GC, we found 55% and 62% were positive for ALDH1 and CD44, respectively, and stained cancer cells of these markers were frequently observed in a wide sphere of tumor lesions. Compared with these markers, only 9% were CD133-positive cases, and CD133-positive cancer cells were observed less-frequently (10–40%) and in a narrower range of lesions. It has been reported that CSCs occupies less than a few percent of whole number of cancer cells.[2,20,32] Therefore, it could be speculated that all markers examined in this present study labeled a larger cell population with some stem cell-like characteristics. Although these markers have been used to identify and isolate both normal and malignant stem cells in many human organs, the specificity for detecting stem cells remains uncertain. Further work to clarify the CSC-like properties of these subpopulations in GC will aid GC stem cell research.

It is also presumed that CSCs can disseminate from the primary tumor to distant sites.[33] In this study, we examined the expression and distribution of CSC markers in both primary and lymph node metastatic sites of GC, and studied the relationship between CSC marker staining and clinicopathologic characteristics. Although few epithelial cells in non-neoplastic gastric mucosa showed CD44 and CD133 staining and only parietal cells were labeled by ALDH1, strong and extensive staining of CSC markers was found in many GC cases. Moreover, CSC markers-positive cases had significant correlations with advanced T grade, N grade or

Table 4 Association between cancer stem cell (CSC) marker expression and morphology in primary gastric cancer (GC) and metastasis

Intestinal-type	Positive rate	*P*-value*
ALDH1		
Primary	31/37 (85%)	0.13
Metastasis	34/46 (74%)	
CD44		
Primary	22/37 (60%)	0.84
Metastasis	28/46 (62%)	
CD133		
Primary	8/37 (21%)	0.28
Metastasis	6/46 (14%)	
Diffuse-type		*P*-value*
ALDH1		
Primary	23/54 (43%)	<0.001
Metastasis	39/47 (83%)	
CD44		
Primary	30/54 (56%)	0.84
Metastasis	28/47 (60%)	
CD133		
Primary	5/54 (9%)	0.79
Metastasis	3/47 (6%)	
Mixed-type		*P*-value*
ALDH1		
Primary	6/13 (46%)	0.70
Metastasis	4/11 (36%)	
CD44		
Primary	8/13 (61%)	1.00
Metastasis	6/11 (54%)	
CD133		
Primary	1/13 (7%)	–
Metastasis	0/11 (0%)	

*χ^2 test: $P < 0.05$ was considered significant.
ALDH1, aldehyde dehydrogenase 1.

stage. On the other hand, staining with CD44 and CD133 had significant prognostic impact in all analysis conditions (all stages, more than stage II, only stage II and III), and multivariate analysis revealed that CD44 and CD133 expression were independent prognostic factors. Based on these results, worse values OS in CD44- and CD133-positive cases were considered not to be simply because these positive cases contained more advance stages. These results are consistent with previous reports that CSC marker expression is significantly upregulated in some solid carcinomas and are risk factors for worse clinical behavior.[25,26,34] Of three CSC markers, CD44 is well known as a target gene of non-canonical WNT signaling cascade and has been implicated in a wide variety of pathological processes and cancer cell biology, such as invasion metastasis.[35,36] However, with regard to CD133 and ALDH1, details of associated functions involving not only CSCs but also normal cells are unclear. In this present study, we found that the positivity of ALDH1 in diffuse-type lymph node metastasis was significantly higher than that of the primary tumor. In diffuse-type GC, it has been reported that transforming growth factor-β (TGF-β) signaling directly represses the transcription of ABCG2, which was used to identify SP cells and negatively contributes to the maintenance of CSCs within the cancer.[37] However, it is well-known that ABCG2 is not directly involved in the tumor-forming ability of SP cells.[38] A correlation between TGF-β signaling and CSC remains obscure. Some recent studies have shown that combination analyses of multiple CSC markers can further restrict the phenotypic definition of CSCs and isolate an even more tumorigenic subset.[17,19] To shed light on the function of ALDH1 and CD133 in cancer tissue, it is necessary to investigate mutual interactions of these CSC marker molecules and study whether CD133 and ALDH1 are involved in WNT or TGF-β signaling, which would help to identify cells of multiple CSC phenotypes.

In summary, we demonstrated the staining properties of CSC markers in normal, metaplastic and cancerous tissue of the stomach. The CSC markers were associated with tumor progression. Both CD44 and CD133 are independent markers for poor survival in patients with GC. However, the detailed functions of CD133 and ALDH1 in GC remain unclear. Clarification of the correlation among these CSC markers may lead to the identification of essential CSC features.

ACKNOWLEDGMENTS

We thank Mr Shinichi Norimura for excellent technical assistance and advice. We also thank the Analysis Center of Life Science, Hiroshima University, for the use of their facilities. This work was supported in part by Grants-in-Aid for Cancer Research from the Ministry of Education, Culture, Science, Sports, and Technology of Japan; in part by Grants-in-Aid for the Third Comprehensive 10-Year Strategy for Cancer Control and for Cancer Research from the Ministry of Health, Labour and Welfare of Japan.

REFERENCES

1 Ohgaki H, Matsukura N. Stomach cancer. In: Stewart BW, Kleihues P, eds. *World Cancer Report.* Lyon: IARC Press, 2003; 197.
2 Reya T, Morrison SJ, Clarke MF, Weissman IL. Stem cells, cancer, and cancer stem cells. *Nature* 2001; **414**: 105–11.
3 Clark MF, Fuller M. Stem cells and cancer: Two faces of eve. *Cell* 2006; **124**: 1111–15.
4 Visvader JE, Lindeman GJ. Cancer stem cells in solid tumours: Accumulating evidence and unresolved questions. *Nat Rev Cancer* 2008; **8**: 755–68.
5 Singh SK, Hawkins C, Clarke ID *et al.* Identification of human brain tumour initiating cells. *Nature* 2004; **432**: 396–401.
6 Ricci-Vitiani L, Lombardi DG, Pilozzi E *et al.* Identification and expansion of human colon-cancer-initiating cells. *Nature* 2007; **445**: 111–5.

7 Singh SK, Clarke ID, Terasaki M *et al.* Identification of a cancer stem cell in human brain tumors. *Cancer Res* 2003; **63**: 5821–8.
8 Ishigami S, Ueno S, Arigami T *et al.* Prognostic impact of CD133 expression in gastric carcinoma. *Anticancer Res* 2010; **30**: 2453–7.
9 Zhao P, Li Y, Lu Y. Aberrant expression of CD133 protein correlates with Ki-67 expression and is a prognostic marker in gastric adenocarcinoma. *BMC Cancer* 2010; **10**: 218–23.
10 Nagano O, Murakami D, Hartmann D *et al.* Cell-matrix interaction via CD44 is independently regulated by different metalloproteinases activated in response to extracellular Ca(2+) influx and PKC activation. *J Cell Biol* 2004; **165**: 893–902.
11 Vigetti D, Viola M, Karousou E *et al.* Hyaluronan-CD44-ERK1/2 regulate human aortic smooth muscle cell motility during aging. *J Biol Chem* 2008; **283**: 4448–58.
12 Aruffo A, Stamenkovic I, Melnick M, Underhill CB, Seed B. CD44 is the principal cell surface receptor for hyaluronate. *Cell* 1990; **61**: 1303–13.
13 Al-Hajj M, Wicha MS, Benito-Hernandez A, Morrison SJ, Clarke MF. Prospective identification of tumorigenic breast cancer cells. *Proc Natl Acad Sci U S A* 2003; **100**: 3983–8.
14 Yasui W, Kudo Y, Naka K *et al.* Expression of CD44 containing variant exon 9 (CD44v9) in gastric adenomas and adenocarcinomas: Relation to the proliferation and progression. *Int J Oncol* 1998; **12**: 1253–8.
15 Collins AT, Berry PA, Hyde C, Stower MJ, Maitland NJ. Prospective identification of tumorigenic prostate cancer stem cells. *Cancer Res* 2005; **65**: 10946–51.
16 Li C, Heidt DG, Dalerba P *et al.* Identification of pancreatic cancer stem cells. *Cancer Res* 2007; **67**: 1030–7.
17 Dalerba P, Dylla SJ, Park IK *et al.* Phenotypic characterization of human colorectal cancer stem cells. *Proc Natl Acad Sci U S A* 2007; **104**: 10158–63.
18 Takaishi S, Okumura T, Tu S *et al.* Identification of gastric cancer stem cells using the cell surface marker CD44. *Stem Cells* 2009; **27**: 1006–20.
19 Ginestier C, Hur MH, Charafe-Jauffret E *et al.* ALDH1 is a marker of normal and malignant human mammary stem cells and a predictor of poor clinical outcome. *Cell Stem Cell* 2007; **1**: 555–67.
20 Huang EH, Hynes MJ, Zhang T *et al.* Aldehyde dehydrogenase 1 is a marker for normal and malignant human colonic stem cells (SC) and tracks SC overpopulation during colon tumorigenesis. *Cancer Res* 2009; **69**: 3382–9.
21 Moreb J, Schweder M, Suresh A, Zucali JR. Overexpression of the human aldehyde dehydrogenase class I results in increased resistance to 4-hydroperoxycyclophosphamide. *Cancer Gene Ther* 1996; **3**: 24–30.
22 Liang D, Shi Y. Aldehyde dehydrogenase-1 is a specific marker for stem cells in human lung adenocarcinoma. *Med Oncol* (in press).
23 Jiang F, Qiu Q, Khanna A *et al.* Aldehyde dehydrogenase 1 is a tumor stem cell-associated marker in lung cancer. *Mol Cancer Res* 2009; **7**: 330–8.
24 Oue N, Mitani Y, Aung PP *et al.* Expression and localization of Reg IV in human neoplastic and non-neoplastic tissues: Reg IV expression is associated with intestinal and neuroendocrine differentiation in gastric adenocarcinoma. *J Pathol* 2005; **207**: 185–98.
25 Kojima M, Ishii G, Atsumi N *et al.* Immunohistochemical detection of CD133 expression in colorectal cancer: A clinicopathological study. *Cancer Sci* 2008; **99**: 1578–83.
26 Shimada Y, Ishii G, Nagai K *et al.* Expression of podoplanin, CD44, and p63 in squamous cell carcinoma of the lung. *Cancer Sci* 2009; **100**: 2054–9.
27 Jiang F, Qiu Q, Khanna A *et al.* Aldehyde dehydrogenase 1 is a tumor stem cell-associated marker in lung cancer. *Mol Cancer Res* 2009; **7**: 330–8.
28 Harn HJ, Ho LI, Chang JY *et al.* Differential expression of the human metastasis adhesion molecule CD44V in normal and carcinomatous stomach mucosa of Chinese subjects. *Cancer* 1995; **75**: 1065–71.
29 Du L, Wang H, He L *et al.* CD44 is of functional importance for colorectal cancer stem cells. *Clin Cancer Res* 2008; **14**: 6751–60.
30 Clevers H. The cancer stem cell: Premises, promises and challenges. *Nat Med* 2011; **17**: 313–9.
31 Mills JC, Shivdasani RA. Gastric epithelial stem cells. *Gastroenterology* 2011; **140**: 412–24.
32 Lee CJ, Li C, Simeone DM. Human pancreatic cancer stem cells: Implications for how we treat pancreatic cancer. *Transl Oncol* 2008; **1**: 14–8.
33 Pantel K, Alix-Panabières C, Riethdorf S. Cancer micrometastases. *Nat Rev Clin Oncol* 2009; **6**: 339–51.
34 Charafe-Jauffret E, Ginestier C, Iovino F *et al.* Aldehyde dehydrogenase 1-positive cancer stem cells mediate metastasis and poor clinical outcome in inflammatory breast cancer. *Clin Cancer Res* 2010; **16**: 45–55.
35 Ponta H, Sherman L, Herrlich A. CD44: From adhesion molecules to signalling regulators. *Nat Rev Mol Cell Biol* 2003; **4**: 33–45.
36 Ishimoto T, Oshima H, Oshima M *et al.* CD44+ slow-cycling tumor cell expansion is triggered by cooperative actions of Wnt and prostaglandin E2 in gastric tumorigenesis. *Cancer Sci* 2010; **101**: 673–8.
37 Ehata S, Johansson E, Katayama R *et al.* Transforming growth factor-β decreases the cancer-initiating cell population within diffuse-type gastric carcinoma cells. *Oncogene* 2011; **30**: 1693–705.
38 Patrawala L, Calhoun T, Schneider-Broussard R, Zhou J, Claypool K, Tang DG. Side population is enriched in tumorigenic, stem-like cancer cells, whereas ABCG2+ and ABCG2- cancer cells are similarly tumorigenic. *Cancer Res* 2005; **65**: 6207–19.

Deficiency of Claudin-18 Causes Paracellular H^+ Leakage, Up-regulation of Interleukin-1β, and Atrophic Gastritis in Mice

DAISUKE HAYASHI,*,‡ ATSUSHI TAMURA,* HIROO TANAKA,* YUJI YAMAZAKI,* SHIN WATANABE,* KOYA SUZUKI,* KAZUO SUZUKI,§ KAZUHIRO SENTANI,‖ WATARU YASUI,‖ HIROMI RAKUGI,‡ YOSHITAKA ISAKA,‡ and SACHIKO TSUKITA*

*Laboratory of Biological Science, Graduate School of Frontier Biosciences and Graduate School of Medicine, and ‡Department of Geriatric Medicine and Nephrology, Graduate School of Medicine, Osaka University, Osaka; §Department of Immunology, Graduate School of Medicine, Chiba University, Chiba; and ‖Department of Molecular Pathology, Hiroshima University Graduate School of Biomedical Sciences, Hiroshima, Japan

See the Covering the Cover synopsis on page 192.

BACKGROUND & AIMS: Although defects in tight junction (TJ) epithelial paracellular barrier function are believed to be a primary cause of inflammation, the mechanisms responsible remain largely unknown. **METHODS:** We generated knockout mice of stomach-type claudin-18, a major component of TJs in the stomach. **RESULTS:** *Cldn18*$^{-/-}$ mice were afflicted with atrophic gastritis that started on postnatal day 3. This coincided with a decrease in intragastric pH due to H^+ secretion from parietal cells and concomitant up-regulation of the cytokines, interleukin-1β, cyclooxygenase-2, and KC, resulting in spasmolytic polypeptide-expressing metaplasia (SPEM). Oral administration of hydrochloric acid on postnatal day 1 induced the expression of these cytokines in *Cldn18*$^{-/-}$ infant stomach, but not in *Cldn18*$^{+/+}$ mice. A paracellular H^+ leak in *Cldn18*$^{-/-}$ stomach was detected by electrophysiology and H^+ titration, and freeze-fracture electron microscopy showed structural defects in the TJs, in which the tightly packed claudin-18 (stomach-type)-based TJ strands were lost, leaving a loose meshwork of strands consisting of other claudin species. **CONCLUSIONS: These findings provide evidence that claudin-18 normally forms a paracellular barrier against H^+ in the stomach and that its deficiency causes paracellular H^+ leak, a persistent up-regulation of proinflammatory cytokines, chronic recruitment of neutrophils, and the subsequent development of SPEM in atrophic gastritis.**

Keywords: Claudin; Gene Knockout; Tight Junction; Gastritis.

The epithelial system defines the parameters of biological homeostasis in multicellular organisms, including the immunologic defense system.[1,2] Epithelial cells adhere to each other to form cell sheets, and when the intercellular spaces between epithelial cells are sealed by tight junctions (TJs), the paracellular barrier function is established.[3–7] The gastric epithelia are specifically resistant to hazardous materials, such as strong acids and the protease pepsin.[8] Defects in these security systems are assumed to cause diseases such as gastritis.[8–10] Chronic gastritis is a risk factor for gastric cancer, and a major cause of gastritis is infection by *Helicobacter pylori*.[11–14] Specific inflammation-related interleukins (ILs), tumor necrosis factor (TNF)-α, interferons, and prostaglandins are reportedly involved in the recruitment of inflammatory cells to chronically inflamed tissue.[15,16] On the other hand, the cell-cell adhesion system that typifies epithelial cell sheets may be important in establishing a bulwark against gastric inflammation.[17–19]

In epithelial cell sheets, the TJ system is primarily responsible for establishing the paracellular barrier function.[20,21] The TJ is a supramolecular complex in which combinations of several kinds of transmembrane proteins, including claudins, TAMPs, and JAMs, are associated with membrane-scaffolding proteins such as ZO-1/2 and cingulin,[22–24] allowing the dynamic regulation of ion and solute passage across the paracellular space. Among the TJ proteins, claudins are specifically required to form the TJ strands that organize the paracellular barrier structure.[3,4,25,26] The multi-gene claudin family has at least 27 members in human/mouse.[3,27] Although claudins are paracellular barrier-forming proteins, there do exist "ion-leaky" claudins that allow specific ions to cross the barrier.[26,28–30] One of the most remarkable characteristics of claudin family proteins is their distinct, tissue function-dependent expression patterns.[27,31]

Claudin-18 has two alternative splicing forms, the lung and stomach types, which use a different first exon and the same exons 2–4; the two isoforms are regulated by different tissue-specific promotors.[32] Because the stomach-type claudin-18 is the predominant claudin expressed in stomach, it is expected to regulate the stomach-specific properties of the paracellular barrier, including resistance to H^+ leakage and/or pepsin, as implied by its overexpression in MDCK II cells.[19] In this study, to understand the role of stomach-type claudin-18 in gastric epithelia, we generated and analyzed knockout mice of stomach-type claudin-18 (*Cldn18*$^{-/-}$ mice).

Abbreviations used in this paper: COX, cyclooxygenase; IF, intrinsic factor; IL, interleukin; qRT-PCR, quantitative real-time polymerase chain reaction; SPEM, spasmolytic polypeptide-expressing metaplasia; TJ, tight junction; TNF, tumor necrosis factor.

0016-5085/$36.00
doi:10.1053/j.gastro.2011.10.040

Using electrophysiologic, H^+-titrational measurements, and electron microscopic analyses, we found that the TJ-mediated barrier against H^+ leakage was impaired in *Cldn18*$^{-/-}$ stomach. Infant *Cldn18*$^{-/-}$ mice developed atrophic gastritis once the intragastric pH began to decrease. This gastritis involved the up-regulation of IL-1β and a consistent infiltration of neutrophils. Our findings strongly suggest that H^+ leakage across the gastric epithelia was the major cause of gastritis in the *Cldn18*$^{-/-}$ mice. These findings may provide a new paradigm for understanding the regulation of chronic inflammation in general.

Materials and Methods

Generation of Cldn18$^{-/-}$ *Mice and Histology*

The targeting vector was constructed as shown (Figure 1). Animal experiments were performed as previously described.[30,33-35]

Antibodies

The primary antibodies for intrinsic factor (IF) was generously provided by Drs J. Mills and D. Alpers[36,37] and for E-cadherin antibody was generously provided by Dr M. Takeichi. All other antibodies used are described in Supplementary Materials and Methods.

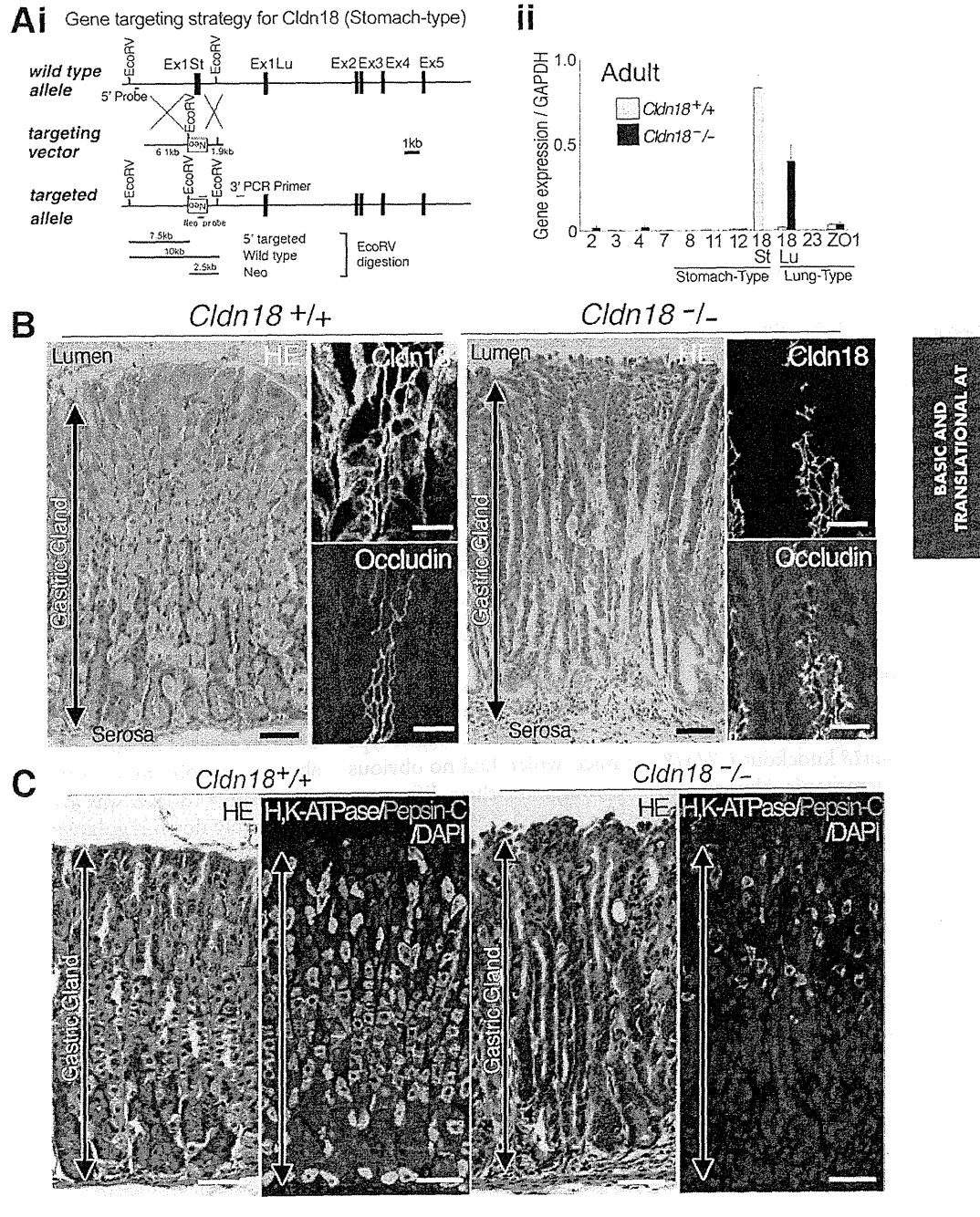

Figure 1. Generation of stomach-type claudin-18 knockout mice. (*A* [*i*]) Construction of the wild-type allele, targeting vector, and targeted allele of the mouse claudin-18 gene. (*A* [*ii*]) Gene expression of claudin family members in *Cldn18*$^{+/+}$ and *Cldn18*$^{-/-}$ adult stomach, as determined by qRT-PCR ($n \geq 4$). (*B*) Light microscopic images of H&E-stained paraffin sections and immunofluorescence of frozen sections of *Cldn18*$^{+/+}$ and *Cldn18*$^{-/-}$ stomach for claudin-18 and occludin. *Bars* = 50 μm (color panels) and 20 μm (gray panels). (*C*) Light microscopic images of H&E-stained paraffin sections and immunofluorescence images of sections stained with antibodies against H^+,K^+-ATPase (H,K-ATPase) and pepsin C. *Bars* = 50 μm.

Electrophysiology and Proton, Biotin, and Dextran Permeation Assays

The conductance, dilution potential, and permeability of H^+ and dextran were measured using an Ussing 2-chamber apparatus.[19,30,38] Biotin permeation was measured by previously described methods.[33]

Gene Expression Assays and Measurement of Cytokine Levels by Enzyme-Linked Immunosorbent Assay

Quantitative real-time polymerase chain reaction (qRT-PCR) was performed as described previously (Supplementary Table 1).[33] The levels of IL-1β and IL-6 in *Cldn18*$^{+/+}$ and *Cldn18*$^{-/-}$ mouse serum were determined using an enzyme-linked immunosorbent assay kit (BD Biosciences, NJ).

Single Cell Preparation and Fluorescence-Activated Cell Sorter Analysis

Stomach samples were processed as previously described but with slight modifications.[39]

Ultrathin-Section Electron Microscopy and Freeze-Fracture Replica Electron Microscopy

Samples were processed as previously described in the Supplementary Materials and Methods Section.[33]

Statistical Analysis

Results are expressed as means ± SEM. P values were calculated using an independent t test, with $P < .05$ considered significant.

See Supplementary Materials and Methods for more details.

Results

Generation of Stomach-Type Claudin-18 Knockout Mice

Two splicing forms of claudin-18, stomach-type variant 2 and lung-type variant 1, are the respective predominant claudins in mouse stomach and lung (Figure 1*A* and Supplementary Figure 1). In adult stomach, there were low levels of all the claudins except claudin-18, including claudin-2, -3, -4, -7, -8, -11, -12, and -23, as shown by quantitative assessment of their messenger RNAs (Figure 1*A*). Here, we generated stomach-type *Cldn18* knockout (*Cldn18*$^{-/-}$) mice, which had no obvious macroscopic abnormalities throughout their life span (data not shown).

In adult *Cldn18*$^{-/-}$ stomach, although lung-type claudin-18 was up-regulated, as shown by qRT-PCR (Figure 1*A* and Supplementary Figure 1), the presence of gastritis indicates that this did not compensate for the loss of stomach-type claudin-18. The staining distributions of the two types of claudin-18 was different; the stomach type was expressed in the TJ/lateral membrane and the lung type in the TJs (see Figure 1*B* and Supplementary Figure 2). Furthermore, there was a slight difference in the distribution and expression level of claudin-2 between *Cldn18*$^{+/+}$ and *Cldn18*$^{-/-}$ stomach in adults (Supplementary Figure 2), similar messenger RNA and protein expression levels of occludin in both infant and adult Cldn18$^{+/+}$ and Cldn18$^{-/-}$ stomach, and a slight decrease in the tight junctional localization of Cldn18$^{-/-}$ adult superficial mucous epithelial cells (Supplementary Figure 3). No obvious changes in the levels of other cell-cell adhesion-related proteins were found between the *Cldn18*$^{+/+}$ and *Cldn18*$^{-/-}$ stomach (Supplementary Figure 2*A*).

Characterization of Gastritis in Stomach-Type Claudin-18 Knockout Mice

Tissue-level examination revealed chronic gastritis in adult *Cldn18*$^{-/-}$ stomach (Figure 1*B* and *C* and Supplementary Figure 4). In H&E-stained preparations, the gastric gland of adult *Cldn18*$^{+/+}$ mice showed typical cell type distribution, with parietal cells predominant at the midlevel region and chief cells predominant at the basal region. In contrast, in *Cldn18*$^{-/-}$ stomach, there were far fewer parietal and chief cells, which had largely been replaced by metaplastic cells with dilated gland lumina (Figure 1*B* and *C* and Supplementary Figures 4 and 5). Furthermore, inflammatory cells were abundant in the *Cldn18*$^{-/-}$ submucosal region. Finally, the incidence of gastritis was 100% in *Cldn18*$^{-/-}$ mice.

Close examination of H&E-stained samples and sections immunostained with specific markers for parietal (anti-H^+,K^+-adenosine triphosphatase [ATPase]) and chief cells (anti-pepsin C/anti-IF) showed that their numbers, as well as that of mature surface mucous cells, were lower than normal in the *Cldn18*$^{-/-}$ gastric mucosa, which was consistent with the difference we observed in the position of the Ki-67–positive proliferative zone (Supplementary Figure 6). These findings were confirmed by qRT-PCR experiments that showed down-regulation of H^+,K^+-ATPase, IF, and MUC5AC (Supplementary Figure 7).

Down-regulation of Claudin-18 Expression in Human Gastric Metaplasia

Because previous studies reported the down-regulation of claudin-18 expression in human gastric cancer,[40] we investigated the expression levels of claudin-18 in human chronic and autoimmune gastritis by an immunohistochemical survey. We found that claudin-18 was down-regulated in human gastritis specimens at foci that showed atrophy and metaplasia. In superficial gastritis, the claudin-18 level was also decreased. Thus, claudin-18 is probably down-regulated pathologically in human gastritic tissue (Figure 2 and Supplementary Figure 8), suggesting that mouse *Cldn18*$^{-/-}$ gastritis may be a good model system for human disease.

Changes in the TJ Strands of Claudin-18–Deficient Mice

Because claudin-18 is the major TJ component of stomach epithelial cells, we examined TJ morphology by electron microscopy (Figure 3). In *Cldn18*$^{+/+}$ stomach at low magnification, well-differentiated parietal cells and chief cells around the lumen of the gland were visible. In contrast, spasmolytic polypeptide-expressing metaplasia (SPEM) cells were dominant in *Cldn*18$^{-/-}$ stomach, with few number of

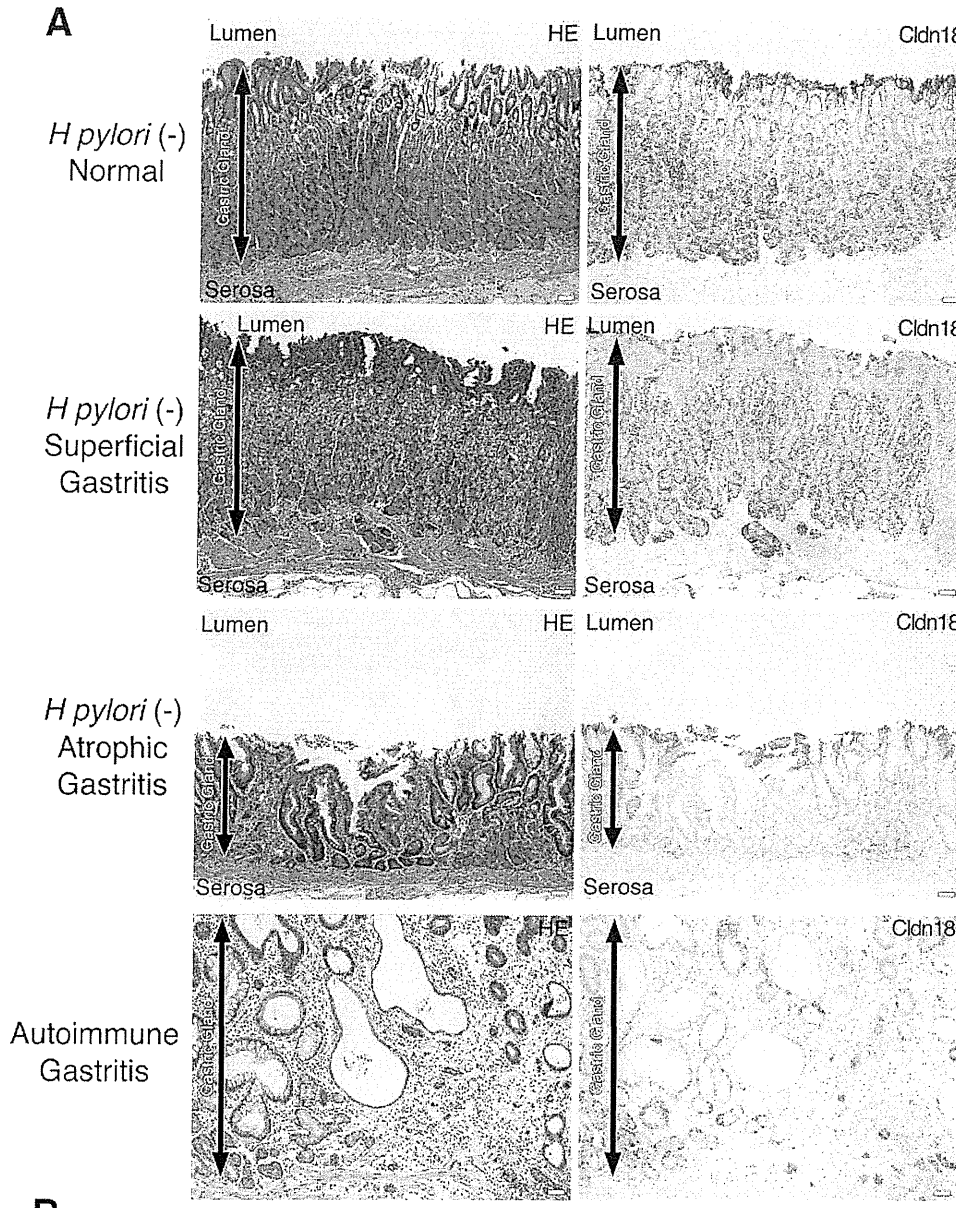

B

Expression of Cldn18 (0 ~ 4+)	4+	3+	2+	1+	0
Normal (n=9)	9 (100%)	0	0	0	0
Chronic superficial gastritis (n=28)	19 (68%)	8 (29%)	1 (4%)	0	0
Chronic atrophic gastritis (n=37)	3 (8%)	6 (16%)	15 (41%)	12 (32%)	1 (3%)
Intestinal metaplasia (n=41)	0	0	2 (5%)	22 (54%)	17 (41%)

Expression of Cldn18

4+ ; 75-100%
3+ ; 50-75%
2+ ; 25-50%
1+ ; 1-25%
0 ; 0%

Figure 2. Human gastritis studies show a down-regulation of stomach-type claudin-18. (*A*) H&E-stained and immunohistochemically claudin-18–stained micrographs of paraffin sections from normal and gastritic regions of a human stomach. Claudin-18 is down-regulated in gastritis. (*B*) Statistical information about the expression of claudin-18 in human gastritis. *Bars* = 50 μm.

well-differentiated parietal and chief cells (Figure 3*A*). Additionally, high magnification showed noticeably reduced TJ width in *Cldn18*$^{-/-}$ stomach (Figure 3*B*).

For TJs to exert their barrier function, TJ strands must be formed. In some tissues, the morphology of the TJ strands at least partly reflects the ability of TJs to function. Freeze-fracture electron microscopy showed highly H^+-resistant TJ strands in adult *Cldn18*$^{+/+}$ stomach as double layers. The most apical layer consisted of tightly packed parallel TJ strands, below which was a layer of much more loosely anastomosing strands (Figure 3*C*). In *Cldn18*$^{-/-}$ stomach, the upper layer of the TJ strands was missing, which explained the decreased TJ width in thin-section electron micrographs of *Cldn18*$^{-/-}$ stomach. Considering the predominant expression of claudin-18 in *Cldn18*$^{+/+}$ stomach, the upper layer of tightly packed TJ strands probably consists largely of stomach-type claudin-18 and forms a highly H^+-resistant paracellular bar-

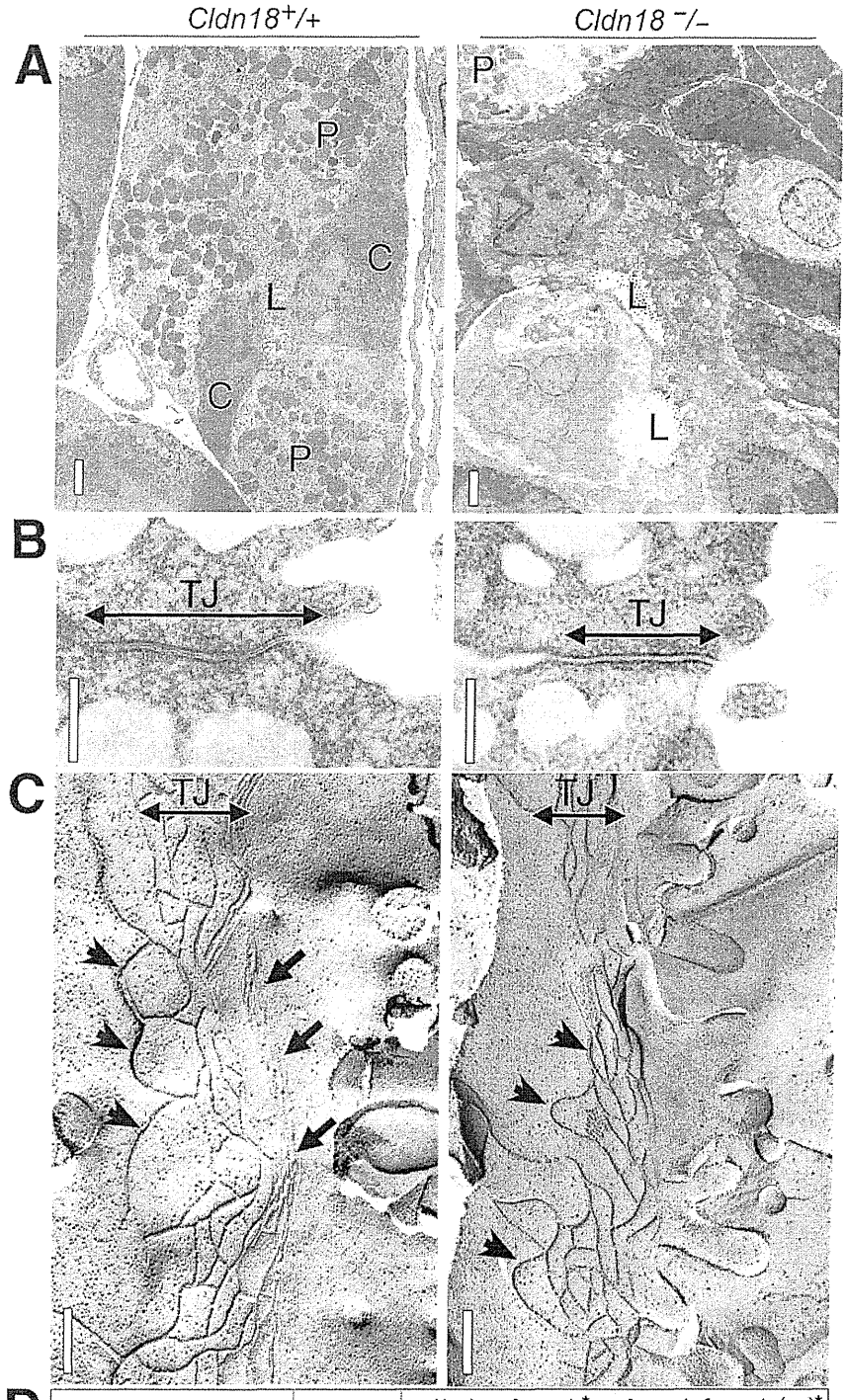

D

		Number of strands*	Interval of strands (nm)*
Packed superior region	Cldn18+/+	3.27±0.23	0.73±0.03
	Cldn18−/−	0.30±0.14	1.12±0.01
		(P<<.01)	(P=.009)
Non packed inferior region	Cldn18+/+	4.60±0.17	4.08±0.22
	Cldn18−/−	4.89±0.30	4.27±0.30
		(P=.41)	(P=.62)

*Intervals and Number of strands on a line drawn perpendicular to the junctional axis. Mean ± SEM.

Figure 3. Electron microscopic characterization of *Cldn18*$^{+/+}$ and *Cldn18*$^{-/-}$ stomach. (*A* and *B*) Thin-section electron microscopic images of TJs in *Cldn18*$^{+/+}$ and *Cldn18*$^{-/-}$ stomach. L, lumen of gastric glands; P, parietal cells; C, chief cells. *Bars* = 1 μm. (*C*) Freeze-fracture electron microscopic images of TJ strands in *Cldn18*$^{+/+}$ and *Cldn18*$^{-/-}$ stomach. Densely packed TJ strands (*arrows*) in the apical region of *Cldn18*$^{+/+}$ gastric epithelial cells were absent in the *Cldn18*$^{-/-}$ cells, which instead showed loosely anastomosing TJ strands (*arrowheads*). *Bars* = 1 μm. (*D*) Statistical information about the numbers and densities of TJ strands in *Cldn18*$^{+/+}$ and *Cldn18*$^{-/-}$ gastric epithelial cells.

rier. The quantification[33] of TJ strands allowed us to estimate an average number of strands to which stomach-type claudin-18 contributes to be approximately 3.0. On the other hand, the lower layer of loosely anastomosing TJ strands may consist of various types of claudins (Figure 3*D*). Together, these results suggest that stomach-type claudin-18 is important for morphologically distinct, parallel, tightly packed TJ strands and that TJ strands in the stomach may functionally specialize to create a paracellular barrier against H^+.

Characterization of Gastritis in Cldn18$^{-/-}$ Stomach by Histologic Examination and by Inflammation-Related Biomarkers

The gastric epithelium of *Cldn18*$^{-/-}$ stomach was largely occupied by proliferating mucous-like cells positive for TFF2 (Figure 4*A* and Supplementary Figure 7). Some of these cells were also positive for IF, indicating SPEM[9] (Figure 4). Thus, adult *Cldn18*$^{-/-}$ mouse stomach showed characteristics of atrophic gastritis, an interpretation supported by the down-regulation of genes for H^+,K^+-ATPase and IF and up-regulation of the TFF2 gene, as assessed by qRT-PCR (Supplementary Figure 7). Finally, HE4,[41] another marker for metaplasia, was also up-regulated, although no cancerous changes were detected histologically (Supplementary Figure 9).

Claudin-18 Deficiency Induced Changes in Inflammation Markers in Cldn18$^{-/-}$ Stomach

Next, to characterize the inflammation induced by claudin-18 deficiency, the expressions of various inflammation markers were examined in adult *Cldn18*$^{+/+}$ and *Cldn18*$^{-/-}$ stomachs. *Cldn18*$^{-/-}$ stomachs had higher expressions of the proinflammatory markers IL-1β and TNF-α (Figure 4*B*). We also found that the levels of the neutrophil chemoattractant KC were significantly higher in the *Cldn18*$^{-/-}$ stomach than the *Cldn18*$^{+/+}$ stomach, by qRT-PCR, with a slight up-regulation in MCP-1. In addition, consistent with the reported role of IL-1β in gastritis, we found that the protein level of serum IL-1β was up-regulated in *Cldn18*$^{-/-}$ mice (Figure 4*B*). Analysis of immune cell types by fluorescence-activated cell sorting revealed that neutrophils, which are positive for Gr-1 and negative for CD11b, predominated in gastritic *Cldn18*$^{-/-}$ tissue (Figure 4*C*). This is in agreement with our finding by immunofluorescence that neutrophils, but not macrophages, significantly increased in *Cldn18*$^{-/-}$ stomach of mice younger than 20 weeks of age (Figure 4*D* and Supplementary Figures 4 and 5).

The expression level of cyclooxygenase (COX)-2 was also higher in *Cldn18*$^{-/-}$ stomach, suggesting the involvement of prostaglandin E_2-related inflammation/restoration reactions (Figure 4*B*). There were no detectable changes in the expression levels of IL-2, IL-4, or IL-6 in the gastritic tissue, however, and no significant changes in the serum level of IL-6, suggesting that B cell and T cell-related immune systems were not significantly involved in this type of gastritis (Supplementary Figure 10).

The changes of tissue constitution associated with gastritis, as detected in *Cldn18*$^{-/-}$ corpus described previously, were not seen in *Cldn18*$^{-/-}$ antrum, consistently with that TFF2 expression was significantly changed in *Cldn18*$^{-/-}$ corpus but not in *Cldn18*$^{-/-}$ antrum. However, the increase in inflammation markers such as IL-1β was similarly induced for *Cldn18*$^{-/-}$ corpus and *Cldn18*$^{-/-}$ antrum. Possibly in this relation, gastrin expression was not up-regulated in the achlorhydric state of *Cldn18*$^{-/-}$ mice (Supplementary Figure 11*E*).

Age of Onset of Gastritis in Cldn18$^{-/-}$ Stomach

To discern the age of onset of gastritis, we first examined stomach specimens histologically. We did not find significant histologic differences between *Cldn18*$^{+/+}$ and *Cldn18*$^{-/-}$ stomachs at postnatal days 1-3 (Figure 5*A*). In postnatal day 4 mice, the number of H^+,K^+-ATPase–positive parietal cells in *Cldn18*$^{-/-}$ stomach showed a slight decrease compared with *Cldn18*$^{+/+}$ stomach. This difference in number became significant at postnatal day 7 (Figure 5*B*). Consistent with these results, qRT-PCR detected a decrease in the expression of H^+,K^+-ATPase and IF in *Cldn18*$^{-/-}$ stomachs (Figure 5*C*).

Acidification of the stomach lumen was detected at postnatal day 3 in *Cldn18*$^{+/+}$ stomach and increased at least until postnatal day 14 (Figure 6). In contrast, although some acidification was detected at postnatal day 3 in *Cldn18*$^{-/-}$ stomach, it did not increase with age, perhaps because of the decrease in total number of parietal cells. Hence, the age of onset of histologic gastritis largely coincided with onset of gastric H^+ secretion in *Cldn18*$^{-/-}$ stomach, suggesting a causal relationship between H^+ secretion and gastritis.

We next examined the levels of inflammation markers at postnatal days 1, 2, 3, and 4 (Figure 6*A*). Beginning at postnatal day 3, IL-1β in *Cldn18*$^{-/-}$ stomach was significantly and constantly up-regulated compared with *Cldn18*$^{+/+}$ (Figure 6). KC was also up-regulated, which was consistent with the neutrophil infiltration associated with *Cldn18*$^{-/-}$ gastritis in infant mice. COX-2 expression changed over the same time course as IL-1β, suggesting that prostaglandin E_2-related inflammation/restoration reactions occurred while IL-1β was up-regulated. Expression levels of TNF-α and MCP-1 tended toward later up-regulation (approximately postnatal day 14), consistent with the inflammation reaction. Markers such as IL-2 and IL-4 were not significantly up-regulated at postnatal days 3 and 4 (data not shown).

Together, these findings point to a role for claudin-18 in forming the H^+-resistant paracellular barrier between stomach epithelial cells and indicate that the barrier prevents gastritis by resisting inflammation. Consequently, defects in the H^+-resistant paracellular barrier caused by deleting claudin-18 result in inflammation induced due to